

Influence of Surface Roughness of Conducting Spheres on the Response of a Phase-Doppler Anemometer

Gerhard Göbel*, Adrian Doicu*, Thomas Wriedt**, Klaus Bauckhage*

(Received: 6 May 1997; resubmitted: 8 September 1997)

Abstract

The influence of the surface roughness of solid conducting spheres on the response of a phase-Doppler anemometer (PDA) is described by using a ray theory model. A rough particle surface is modeled as an ensemble of distorted spheres. First- and second-order reflection and diffraction are considered for far-field

calculations of the PDA phase difference. The numerical simulations are accompanied and supported by experimental results. Single rough Sn spheres are captured inside an electrodynamic trap and investigated with a standard phase-Doppler system.

1 Introduction

Phase-Doppler anemometry (PDA) is a well established technique for determining the size and velocity of spherical particles in various engineering processes. The design of a phase-Doppler system includes simulations based on Mie theory, which describes the scattering of a plane wave by a spherical particle. Although solid particles are usually non-spherical, the real shape is neglected and the particles are assumed to be perfectly spherical. The same holds for real surfaces, e.g. conducting particles with rough surfaces. Experimentally, it was found that the response of a phase-Doppler system deviates from the theoretical prediction when surface roughness is present. The deviation is pronounced with increasing surface distortion. It is therefore necessary to adapt the theories of light scattering by particles that possess a rough surface for PDA calculations.

Scattering by particles with rough surfaces has received considerable attention. For particles with a random shape it is possible to solve Maxwell's equations numerically, realization-by-realization, to find the mean scattered intensity and its statistical properties (e.g. variance). The extended boundary condition method or the method of moments is capable of predicting the angular distribution of the scattered intensity and can be successfully applied for such simulations. *Michel* [1], and *Peltoniemi* [2] have developed a distorted wave approach based on the Dyson and Bethe-Salpeter equations and on a variational volume integral technique, respectively, for light scattering by irregular particles. However, for particles with large size parameters the numerical effort is considerable and generally applicable.

The disadvantage of exact methods is that they give little physical insight into the scattering mechanism behind the resulting scattered intensity distribution. However, approximate methods can give a clear picture of the physical process involved in the scattering. *Bahar* et al. analyzed the scattering cross-sections of

spheres and infinite cylinders with the full wave approach [3,4]. Some researchers also obtained the coherent scattering cross-section by employing perturbation theory [5,6]. For roughness parameters $\beta = 4k^2\delta^2 \ll 1$ (k is the wavenumber in free space and δ is the standard deviation of rough surface heights), perturbation theory can be used to determine the scattering patterns. On the other hand, as β is close to or larger than unity, perturbation theory cannot be applied.

When the radii of curvature of unperturbed particles are much larger than the incident wavelength, the mean square slope of the rough surface is smaller than unity, and when multiple scattering from the particle surface is neglected, then the major contribution to the scattered field comes from the neighborhood of the specular points and the first-order Kirchhoff approximation or the physical optics method can be applied [7]. We note here that for rough surfaces with a mean square slope of the order of unity the second-order Kirchhoff approximation with shadowing corrections was used by *Ishimaru* et al. [8] (to account for multiple scattering on the particle surface). When the stationary phase method is used to evaluate the diffraction integrals derived in the physical optics approximation, one obtains the geometric optics solution. In this context, the contribution of *Muinsonen* et al. [9] dedicated to the ray optics approximation for Gaussian random particles is relevant.

The aim of this paper is to investigate the influence of the particle roughness on the response of a phase-Doppler anemometer. The organization of the paper is as follows. In Section 2 we use the first-order Kirchhoff approximation to derive a simple expression for the phase-Doppler signal. For this purpose we use the stationary-phase method to evaluate the diffraction integrals and assume that there exists only one specular point on the particle surface. In Section 3 we use ray theory to model the phase-Doppler signal. For perfectly conducting particles we generate sample Gaussian random surfaces and compute the far-zone electric field by considering reflection and diffraction. Furthermore, for particles with high surface roughness second-order reflection is taken into account. In Section 4 we support our results with phase-Doppler measurements on individual rough Sn particles. An electrodynamic particle trap is employed for levitation of single charged particles in the size range $5\mu\text{m} < d < 50\mu\text{m}$.

* Dipl.-Phys. G. Göbel, Dr.-Ing. A. Doicu, Prof. Dr.-Ing. K. Bauckhage, Fachgebiet Verfahrenstechnik, Universität Bremen, Badgasteiner Straße 3, 28359 Bremen (Germany).

** Dr.-Ing. T. Wriedt, Institut für Werkstofftechnik, Badgasteiner Straße 3, 28359 Bremen (Germany).

2 Simplified Statistical Characterization of the Random Doppler Signal Phase

The use of the first-order Kirchhoff approximation in PDA modeling leads to a simple expression for the phase difference, which is relevant for practical applications. The following conditions are assumed to be satisfied:

- (Ai) The surface dielectric properties are uniform everywhere, and the rough surface is isotropic in two dimensions.
- (Aii) The radii of principal curvature at any point on the surfaces are much larger than the wavelength and correlation distance.
- (Aiii) The mean square slope is smaller than unity.

These conditions are usually encountered in practice. We consider a perfectly conducting rough sphere with a surface defined in spherical coordinates by

$$r'(\theta, \varphi) = d/2 + \delta f(\theta, \varphi) \tag{1}$$

where d is the mean diameter of the particle, δ is the root mean square value of r' or the standard deviation of the surface heights and $f(\theta, \varphi)$ is a stochastic function of the polar angles θ and φ . The first two moments of $f(\theta, \varphi)$ are given by

$$\langle f(\theta, \varphi) \rangle = 0, \tag{2}$$

$$\langle f(\theta_1, \varphi_1) f(\theta_2, \varphi_2) \rangle = \rho(\gamma)$$

where the angle bracket denotes the average over the ensemble of realizations of the surface profile and $\rho(\gamma)$ is the two-point autocorrelation function which depends only on the angular distance γ between (θ_1, φ_1) and (θ_2, φ_2) .

The particle is illuminated by a monochromatic plane wave traveling in the $\bar{e}_i(\theta_i, \varphi_i)$ direction. The incident magnetic field is written as

$$\bar{H}_0(\bar{r}) = \sqrt{\frac{\epsilon_0}{\mu_0}} E_0 \bar{h}_0 e^{jk\bar{e}_i \cdot \bar{r}} \tag{3}$$

where \bar{h}_0 is the polarization vector, ϵ_0 and μ_0 are the free-space permittivity and permeability, respectively, E_0 is the electric field strength and k is the wavenumber.

In the physical optics approximation, one assumes that the tangential component of the total magnetic field at the particle surface $\bar{n} \times \bar{H}(\bar{r}')$ can be approximated by twice the tangential component of the incident magnetic field $2\bar{n} \times \bar{H}_0(\bar{r}')$, where \bar{n} is the local surface normal. Consequently, the far-zone scattered field is given by

$$\bar{E}(\bar{r}_s) = \frac{e^{jk r_s}}{k r_s} \bar{e}_s \times \bar{e}_s \bar{\mathcal{H}}(\bar{e}_i, \bar{e}_s) \tag{4}$$

where

$$\bar{\mathcal{H}}(\bar{e}_i, \bar{e}_s) = -2jk^2 E_0 (\bar{h}_0 \times \int_S \bar{n} g(\theta, \varphi) e^{jkF(\theta, \varphi)} d\theta d\varphi)$$

$$g(\theta, \varphi) = r'^2 \sin \theta \left(1 + \frac{1}{r'^2} \left(\frac{\partial r'}{\partial \theta} \right)^2 + \frac{1}{r'^2 \sin^2 \theta} \left(\frac{\partial r'}{\partial \varphi} \right)^2 \right)^{1/2}, \tag{5}$$

$$F(\theta, \varphi) = (\bar{e}_i - \bar{e}_s) \cdot \bar{r}'(\theta, \varphi)$$

and $\bar{e}_s(\theta_s, \varphi_s)$ is the unit vector of the scattering direction. The integral is taken over those portions of the surface that are illuminated and in view of the observation point.

The diffraction integral (5) can be evaluated with the stationary-phase method, which leads to the geometric optics solution [10]. For an asymptotic evaluation we expand the integration ranges from $-\infty$ to ∞ so that for sufficiently large k the major contribution to the integral comes from the neighborhood of the stationary-phase points. The stationary points are the roots of the following simultaneous equations:

$$\frac{\partial F(\theta, \varphi)}{\partial \theta} = (\bar{e}_i - \bar{e}_s) \cdot \frac{\partial \bar{r}'}{\partial \theta} = 0$$

$$\frac{\partial F(\theta, \varphi)}{\partial \varphi} = (\bar{e}_i - \bar{e}_s) \cdot \frac{\partial \bar{r}'}{\partial \varphi} = 0.$$

Since Eq. (6) leads to $(\bar{e}_i - \bar{e}_s) \parallel \left(\frac{\partial \bar{r}'}{\partial \theta} \times \frac{\partial \bar{r}'}{\partial \varphi} \right)$, we conclude that in the high frequency limit, the stationary-phase points are the specular points A of angular coordinates (θ_A, φ_A) satisfying

$$\bar{n}_A(\theta_A, \varphi_A) = \frac{\bar{e}_s - \bar{e}_i}{|\bar{e}_s - \bar{e}_i|}. \tag{7}$$

For a convex scatterer, Eq. (6) has only one real root in the illuminated region, whereas for concave-convex particles, several real roots may exist. For concave-convex scatterers, however, one cannot always obtain satisfactory results by taking into account only these real stationary points. Therefore, one should extend the real variables θ and φ into the complex domain and find the complex stationary points in addition to real ones. In order to simplify our presentation we assume that there exists only one real stationary-phase point.

The result of the asymptotic evaluation gives

$$\bar{E}(\bar{r}_s) = \frac{e^{jk r_s}}{k r_s} \bar{E}(\bar{e}_i, \bar{e}_s) e^{j[k(\bar{e}_i - \bar{e}_s) \cdot \bar{r}'_A + \frac{\pi}{2}]} \tag{8}$$

where \bar{r}'_A is the vector at the stationary phase point (specular point), and

$$\bar{E}(\bar{e}_i, \bar{e}_s) = -4\pi j E_0 [\bar{e}_s \times \bar{e}_s \times (\bar{h}_0 \times \bar{n}_A)] \frac{g(\theta_A, \varphi_A)}{\sqrt{|K(\theta_A, \varphi_A)|}} e^{-j\frac{1}{2}\pi \text{arg} K(\theta_A, \varphi_A)}$$

$$K(\theta, \varphi) = F_{\theta\theta} F_{\varphi\varphi} - F_{\theta\varphi}^2, \tag{9}$$

$$F_{\theta\theta} = \partial^2 F / \partial \theta^2, F_{\varphi\varphi} = \partial^2 F / \partial \varphi^2, F_{\theta\varphi} = \partial^2 F / \partial \theta \partial \varphi.$$

For a set of stationary-phase points which are well separated, the asymptotic evaluation of the integral leads to a sum of individual contributions as in Eq. (8). The phase of the scattered field in Eq. (8) corresponds to the dominant reflection mechanism. The vector of the specular point is given by $\bar{r}'_A = (d/2 + \delta f(\theta_A, \varphi_A)) \cdot \bar{e}_{r_A}$, where \bar{e}_{r_A} is the radial unit vector at the point A . If the mean square slope of the particle surface is much smaller than unity, we can consider approximately $\bar{n}_A = \bar{e}_{r_A}$ and, consequently, we obtain the following expression for the phase of the scattered field:

$$\phi = \left[a + \frac{2\delta}{d} f(\theta_A, \varphi_A) \right] \phi_0(\bar{e}_i, \bar{e}_s) + \frac{\pi}{2}, \tag{10}$$

$$\phi_0(\bar{e}_i, \bar{e}_s) = k \frac{d}{2} (\bar{e}_i - \bar{e}_s) \cdot \bar{n}_A = k \frac{d}{2} |\bar{e}_i - \bar{e}_s|.$$

The above relation shows that the statistics of ϕ are given by the statistics of f .

In a PDA system, the particle is illuminated by two incident waves traveling in the \bar{e}_i^1 and \bar{e}_i^2 directions, while the scattered field is analyzed in the \bar{e}_s^α and \bar{e}_s^β directions. The phase difference between the signals of two point detectors is given by

$$\phi_{\alpha\beta} = \phi_{\alpha\beta}^{sphere} + \frac{2\delta}{d} [f(\theta_A^{1\alpha}, \varphi_A^{1\alpha})\phi_0(\bar{e}_i^1, \bar{e}_s^\alpha) - f(\theta_A^{2\alpha}, \varphi_A^{2\alpha})\phi_0(\bar{e}_i^2, \bar{e}_s^\alpha) - f(\theta_A^{1\beta}, \varphi_A^{1\beta})\phi_0(\bar{e}_i^1, \bar{e}_s^\beta) + f(\theta_A^{2\beta}, \varphi_A^{2\beta})\phi_0(\bar{e}_i^2, \bar{e}_s^\beta)] \quad (11)$$

where $\phi_{\alpha\beta}^{sphere}$ is the phase difference which corresponds to an unperturbed sphere of diameter d . Thus, using Eqs. (2) and (11), we conclude that

- (i) the mean of the phase difference is $\langle \phi_{\alpha\beta} \rangle = \phi_{\alpha\beta}^{sphere}$; and
- (ii) the variance of the phase difference $\sigma_\phi^2 = \langle (\phi_{\alpha\beta} - \langle \phi_{\alpha\beta} \rangle)^2 \rangle$ is proportional to $(2\delta/d)^2$.

3 Numerical Simulations

3.1 Numerical Generation of Random Surfaces

In our numerical experiments we generate sample spheres with a Gaussian random rough surface. We assume an axisymmetric roughness, i.e.

$$r'(\theta) = d/2 + \delta f(\theta) \quad (12)$$

in order to reduce the computation time. The particle shape can be generated using Fourier expansions for the radius and the autocorrelation function

$$f(\theta) = \sum_{n \geq 0} a_n \cos(n\theta) + b_n \sin(n\theta) \quad (13)$$

$$\rho(\gamma) = \rho(\theta_1 - \theta_2) = \langle f(\theta_1)f(\theta_2) \rangle = \sum_{n \geq 0} (2 - \delta_{n,0})\rho_n \cos(n\gamma)$$

where $\delta_{n,0}$ is the Kronecker symbol. The particle geometry is depicted in Figure 1.

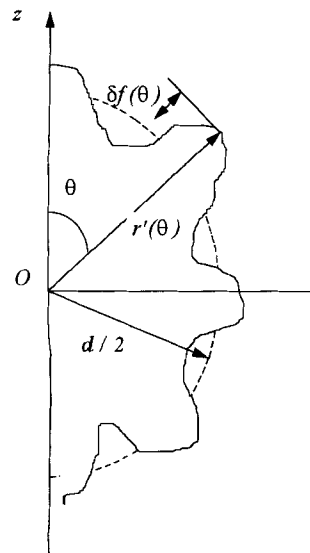


Fig. 1: Particle geometry.

It can be shown that, if the coefficients a_n and b_n are independent Gaussian random variables with zero means and equal variances $\sigma_n^2 = (2 - \delta_{n,0})\rho_n$, the radius will be normally distributed with a mean value of $d/2$ and an autocorrelation function of $\delta^2\rho$. A convenient choice for the autocorrelation function is the spherical ‘‘Gaussian’’ function

$$\rho(\gamma) = e^{-\frac{\delta}{\gamma_c} \sin^2(\gamma/2)} \quad (14)$$

where γ_c represents an angular decay length. Its value must be greater than $2\delta/d$. The expansion coefficients ρ_n are given by

$$\rho_n = e^{-\frac{\delta}{\gamma_c} J_n^2} J_n \left(-j \frac{2}{\gamma_c} \right). \quad (15)$$

The stochastic shape is thus parametrized by ϕ and γ_c , the standard deviation and the angular roughness scale.

3.2 Numerical Calculations of the Phase-Doppler Signal

For each sample Gaussian random surface we compute the phase-Doppler signal by using ray theory. We extend our geometric optics model for PDA calculations [11] to rough particles. For perfectly conducting scatters the far-zone electric field is derived for diffraction and reflection. Diffraction plus reflection was exactly soluble for a spheroidal particle, in the sense that the magnitude, phase and polarization of the electric field of the outgoing rays were directly expressible in terms of the scattering angles. This is not the case for a sphere with an axisymmetric surface roughness. The reflected field sums the contributions of rays which emerge from the specular points. The angular coordinates of a specular point are obtained by solving the vector equation $\bar{n}(\theta_A, \varphi_A) = (\bar{e}_i - \bar{e}_s)/|\bar{e}_i - \bar{e}_s|$ numerically. When the radii of curvature at any point on the surface are comparable to the incident wavelength and the correlation distance, the second-order reflection at the particle surface must be considered [7,8]. In this case a double-scattering ray emerging from a point A will be taken into account if we find a second point A' , visible from A , such that

$$\bar{n}(\theta_A, \varphi_A) = (\bar{e}_s - \bar{e}_{AA'})/|\bar{e}_s - \bar{e}_{AA'}| \quad (16)$$

$$\bar{n}(\theta'_A, \varphi'_A) = (\bar{e}_{AA'} - \bar{e}_i)/|\bar{e}_{AA'} - \bar{e}_i|, \quad \bar{e}_{AA'} = (\bar{r}'_A - \bar{r}'_{A'})/|\bar{r}'_A - \bar{r}'_{A'}|.$$

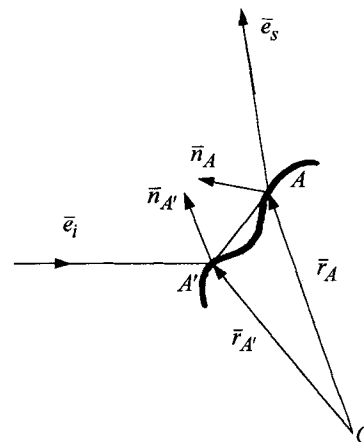


Fig. 2: Geometry of the second-order reflection point on the particle surface.

The meaning of the second-order reflection points can be understood from Figure 2.

The sample size is chosen by imposing that the relative error in estimating the mean phase difference is less than 1% with 95% confidence. Typically, the number of samples is a few hundred, although an appreciable numerical convergence of the averages is usually obtained within 100 samples, or even less. In fact, this method permits one to calculate in a straightforward way any statistical moment of the phase difference. Furthermore, surfaces with other statistics can be similarly studied.

3.3 Numerical Results

An optical configuration with a beam intersection angle of 4° , an off-axis angle of 40° and an elevation angle of 8.7° is considered, in accordance with the experimental setup in Section 4. The receiving-cone angle is taken to be 5° . This corresponds to the setup applied for the experimental investigations. We compute the phase differences for rough spheres with $d = 18 \mu\text{m}$, standard deviations of the surface heights $\delta = 0.1, 0.2, 0.3, 0.4, 0.5$ and $0.6 \mu\text{m}$ and angular roughness scale $\gamma_c = 0.5, 0.6$ and 0.7 .

Figure 3 shows the phase distributions for three values of the radius standard deviation, $\delta = 0.1, 0.3$ and $0.5 \mu\text{m}$. As expected, the increase in the standard deviations introduces more pronounced fluctuations on the phase difference distribution.

We systematically study the influence of δ and γ_c on the standard deviation of the signal phase difference. The results are plotted in Figure 4. For increasing standard deviation δ , the standard deviation of the phase distribution increases. The dependence is approximately linear. The standard deviation of the phase is rather insensitive to changes in the angular roughness scale γ_c .

We then compute the sample mean of the signal phase difference. The data are presented in Figure 5, where the angular roughness scale is chosen as a parameter. The discrepancies between the values of the mean phase for a disturbed sphere and an unperturbed sphere become larger for large values of δ . However, the relative errors are less than 1.5%.

The above numerical analysis demonstrates the validity of the results in Section 2, i.e. for rough spheres with moderate values of the surface slopes, (i) the mean phase of the Doppler signal corresponds to that of an unperturbed sphere and (ii) the dependence of the standard deviation of the phase difference on the radius standard deviation is linear. We note here that for Gaussian random particles with small values of the angular roughness scale γ_c , e.g. in the range (0.2, 0.4), the assumptions (Ai)–(Aiii) fail and the above conclusions are not valid.

4 PDA Measurements

4.1 Experimental Set-up

Our experimental set-up consists of a standard PDA system and an electrodynamic particle trap. Both components are described below.

We used a 100 mW Ar^+ laser ($\lambda = 488 \text{ nm}$). A beam splitting configuration was applied by using a radial diffraction grating ($32 \mu\text{m}$ grid separation) and appropriate imaging of the Gaussian beam by means of two lenses. For the measurements presented below we chose a total beam crossing angle of 4° and a beam diameter of $120 \mu\text{m}$. This gives a fringe distance of $7.0 \mu\text{m}$. The polarization of the beams is perpendicular with respect to the mean scattering plane. Two individually mounted photomultiplier tubes

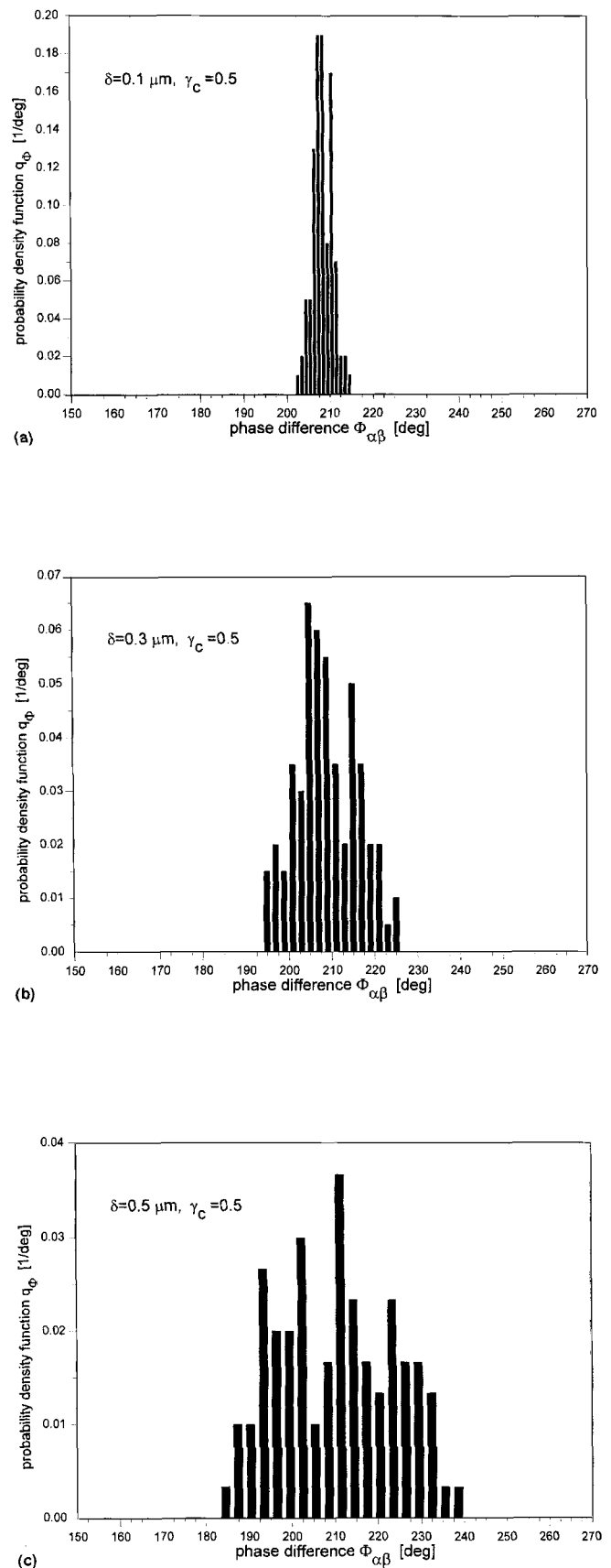


Fig. 3: Numerically simulated phase distributions for a distorted $d = 18 \mu\text{m}$ sphere, an angular roughness scale of $\gamma_c = 0.5$ and standard deviations of surface heights of (a) 0.1, (b) 0.3 and (c) $0.6 \mu\text{m}$.

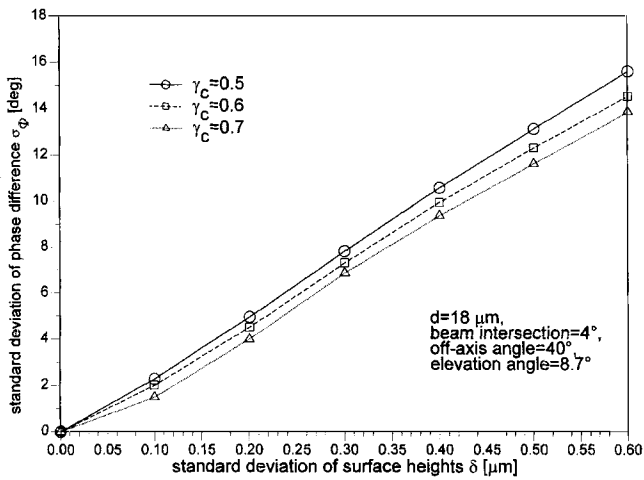


Fig. 4: Standard deviation of phase differences versus standard deviation of surface heights for various angular roughness scales.

(PMTs) are used for detection of the scattered light. Their front lenses are of 52 mm aperture and have a focal length of 300 mm. As we performed measurements on individual particles, no pinholes have to be used for spatial filtering. The PMTs are located at an off-axis angle of 40° under ± 8.7° elevation, yielding a phase sensitivity of 11.17°/μm or a maximum sphere diameter of 32.2 μm. The signals are band-filtered (Krone-Hite analog filters), amplified and digitized with a 12 bit, 30 MHz AD-board from Spectrum, Germany. Data evaluation is performed by means of a standard FFT algorithm. The scheme of the set-up is depicted in Figure 6. Details of the set-up have been published previously [12].

The electrodynamic levitation of individual particles is a well known technique in various disciplines of particle science [13]. The schematic set-up of our ring trap is also depicted in Figure 6. An electrically charged particle is carried against gravity by means of a DC field. A dynamic trapping force is provided by an additional AC field. The trap is built with four ring electrodes, which are arranged in parallel with their centers coinciding with the vertical z-axis of symmetry (direction of gravity). While the end electrodes are supplied with up to 300 V DC voltage, the center electrodes carry an AC voltage (maximum 5 kV, 46 Hz < f_{AC} < 1 kHz) of equal polarity. Both AC and both DC electrodes are identical in size and

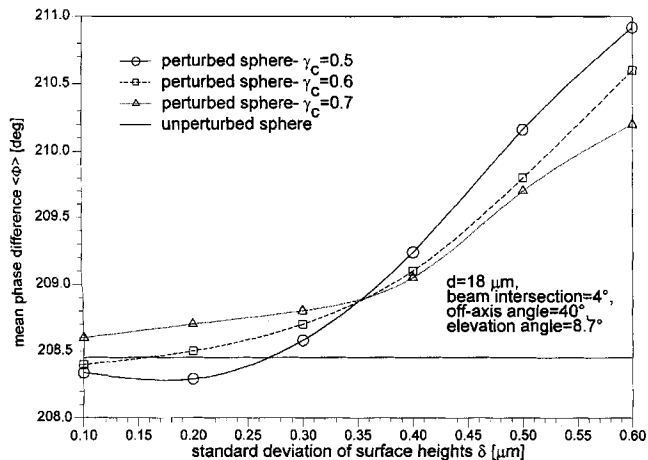


Fig. 5: Dependence of the mean phase difference on the standard deviation of surface heights. Depicted is the exact phase difference of the undistorted sphere and the results for three angular roughness scales.

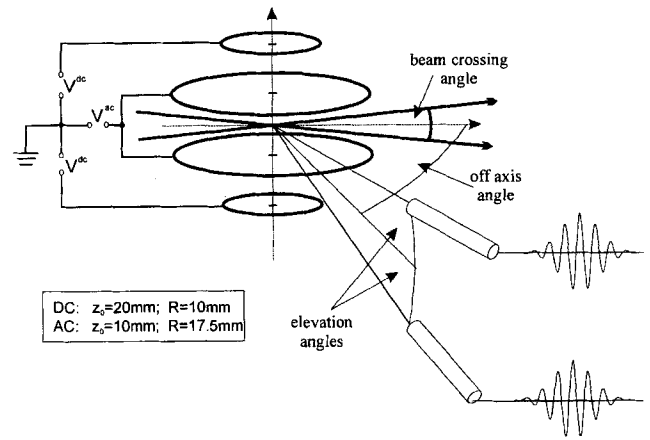


Fig. 6: Scheme of the optical configuration and the electrodynamic particle trap.

they are positioned symmetrically. Solid and fluid particles in the size range 5 μm < d < 50 μm can be carried for hours or even days without difficulty.

Solid particles are charged by frictional electricity with the help of a “plastic” stick. The amount of charge that can be transferred to a particle is limited. A typical value for a 20 μm Sn sphere is approximately 10⁵ elementary charges. The electrical surface properties of the particles strongly influence the charging process.

Once a single particle has been trapped, the electric fields can be adjusted to yield either a motionless fixation or a harmonically oscillating trajectory in the vertical direction with variable amplitude. The latter situation is used in our experiments in order to provide the necessary particle velocity with respect to the beam intersection area. The oscillatory amplitude is chosen clearly larger than the beam diameter (typically 500 μm) in order to prevent large velocity gradients within the measurement volume and thus frequency modulation of the PDA bursts.

After the optical investigation, the levitated particle is captured by means of an electrostatic collector for further characterization in an electron microscope. A REM sample holder coated with conducting glue is supplied with a DC voltage of appropriate polarity and strength. This sample holder is placed just above the upper DC ring of the trap. By a simultaneous and gentle shutdown of the trap voltages and a smooth increase in trapping DC voltage, the levitated particle can easily be captured. The capturing process and the particle trapping procedure can be observed visually via a Questar telescope and a video system.

We should point out that the particle rotates inside the trap during either the oscillation in the vertical direction or the containment. This is obvious from a visual observation with the Questar system, when particles of irregular shape with dimensions clearly larger than the resolution of the Questar (1.5 μm), are levitated. Under these circumstances the whole particle surface will be investigated during the measurement process. Furthermore, we assume that the orientation averaging is equivalent with an averaging over the ensemble of realization of the surface profile.

4.2 Experimental Results

We performed PDA measurements on Sn particles which have been generated by liquid atomization in a standing ultrasonic wave field. Owing to surface tension the particle shape is spherical, but the particle surface exhibits a certain roughness caused by phase

transition processes or mechanical stress prior to complete solidification. The objective of our experiments is to measure the mean diameter of a single rough particle and to give a qualitative description of the particle surface using the roughness parameters of an “equivalent” particle with the same mean diameter and axisymmetric roughness. Particles with $d < 30 \mu\text{m}$ were pre-selected by a sieving process. Typical PDA results for three individual Sn particles are presented here. Figures 7–9 show the number density of phase differences that result from 10^4 phase difference measurements on an identical sphere (512 phase classes for a total of 360°).

Figure 10 shows a electron microscopic photograph of the Sn particle in Figure 7. A closer depiction of the surface structure can be seen in Figure 11. Owing to the high DC voltage during the particle capturing, the particle is submerged in the conducting glue. According to the conclusions of our theoretical analysis, the mean diameter of the particle is given by the sample mean of the phase difference. We found the values $d = 18.67, 18.70$ and $7.12 \mu\text{m}$, respectively. The results are in good agreement with the electron microscopic photograph evaluation and the CCD diffraction readings, the maximal relative error of the mean diameter evaluation being smaller than 2.5%.

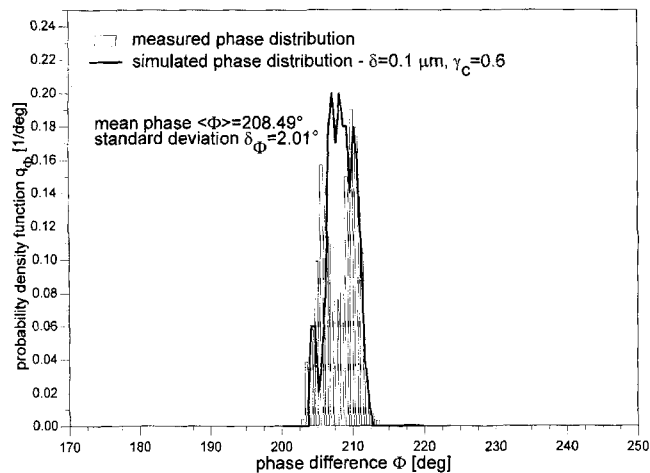


Fig. 7: Measured phase difference distribution for a levitated Sn sphere (10 000 repeated measurements) and numerically simulated phase difference distribution.

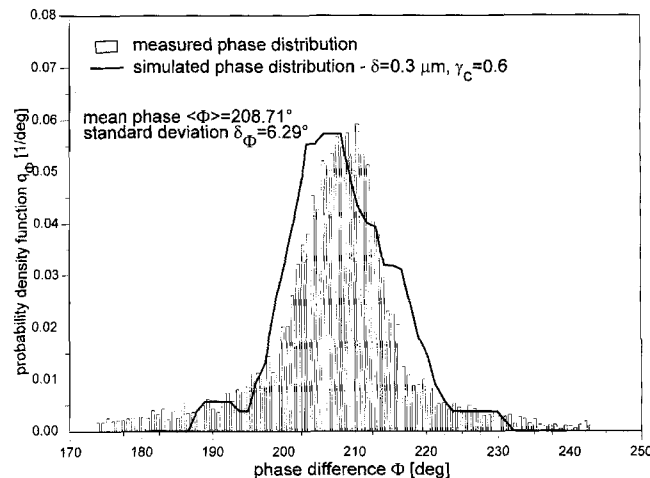


Fig. 8: Measured phase difference distribution for a levitated Sn sphere (10 000 repeated measurements) and numerically simulated phase difference distribution.

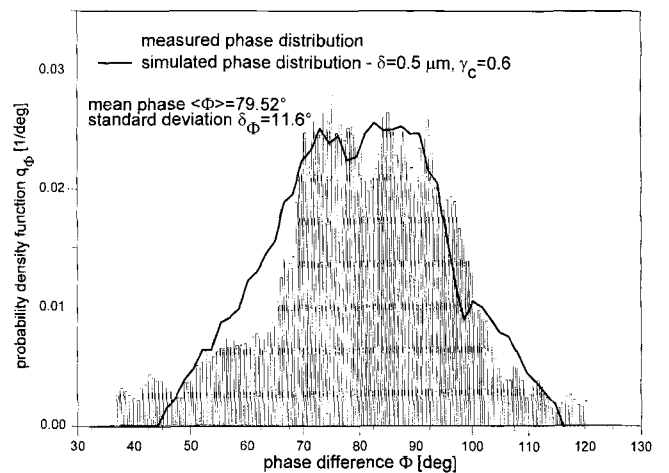


Fig. 9: Measured phase difference distribution for a levitated Sn sphere (10 000 repeated measurements) and numerically simulated phase difference distribution.

The dashed lines in Figures 7–9 represent numerically simulated phase difference distributions from particles with axisymmetric roughness which approximate in the mean square sense the measured phase distributions. We chose the roughness parameters in the ranges $\delta = 0.1, 0.2, \dots, 0.6 \mu\text{m}$ and $\gamma_c = 0.5, 0.6, \dots, 1.0$ and found the optimal values to be $\delta = 0.1, 0.3$ and $0.5 \mu\text{m}$ and $\gamma_c = 0.6$, respectively. This procedure can be regarded as “semi-quantitative” since the roughness parameters correspond to those of an axisymmetric rough particle. However, the “equivalent” roughness parameters can be used as estimators for the real ones. This is supported by an image analysis of a scanned electron microscopic photography. Furthermore, since for particles with small surface slope the influence of the angular roughness scale is not significant, the curves in Figure 4 can be used in order to estimate the standard deviation of the surface heights.

5 Concluding Remarks

This paper has assessed that the response of a phase-Doppler anemometer is very sensitive to the roughness of conducting particles. As an example, we mention here that for a spherical

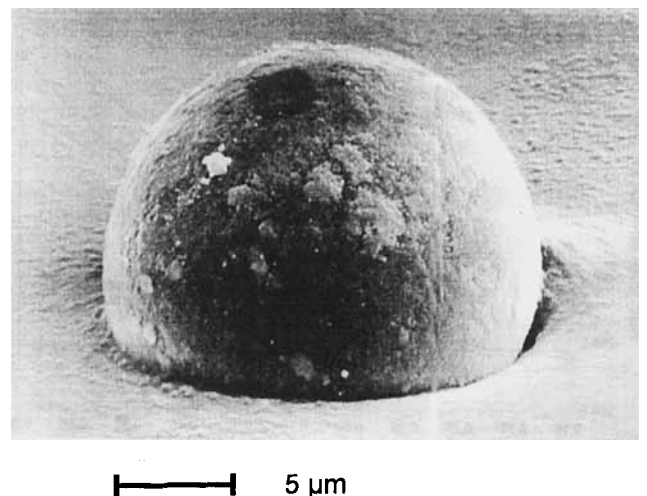


Fig. 10: Electron microscopic photograph of the Sn particle in Figure 7, which was caught after the PDA measurements.



— 2 μm

Fig. 11: REM photograph of the Sn particle surface.

particle with a mean diameter of $d = 18 \mu\text{m}$, the ratio between the standard deviation σ_Φ and the mean value of the phase difference $\langle \Phi \rangle$ increases from 0.01 to 0.077 when the standard deviation of the surface heights δ increases from 0.1 to 0.6 μm . Consequently, for particles with surface heights comparable to the wavelength, the maximal relative error of the phase difference $\varepsilon_\Phi = (3\sigma_\Phi / \langle \Phi \rangle) \cdot 100$ is about 23%.

For particles with moderate values of the surface slope, the mean of the phase difference corresponds to that of an unperturbed sphere and the standard deviation of the phase signal increases linearly with the standard deviation of the surface heights. These results were demonstrated analytically by using a first-order Kirchhoff approximation model for non-axisymmetric particles and verified numerically by using a geometric optics model for axisymmetric particles. Based on the geometric optics model, a ‘‘semi-quantitative’’ procedure for surface roughness evaluation was given.

We regard our results as a first step for further investigations of the particle roughness by the phase-Doppler technique. The use of an electrodynamic levitator in a PDA configuration seems to be a promising method for roughness measurements since the particle rotation offers the possibility of investigating the whole particle surface. In this context, by extending the geometric optics model for computing the scattered light from particles with a non-axisymmetric rough surface it will in principle be possible to determine the real roughness parameters by using the distribution function of the statistical moments of the phase difference.

6 Symbols and Abbreviations

a_n, b_n	random variables with zero mean and equal variance
d	mean diameter of the particle
$\tilde{z}_i(\theta_i, \varphi_i)$	unit vector of the propagation direction of the incident wave
$\tilde{z}_s(\theta_s, \varphi_s)$	unit vector of the scattering direction
E_0	electric field strength
\tilde{E}_s	scattered field
$f(\theta, \varphi)$	stochastic function
\tilde{h}_0	polarization vector of the incident magnetic field
\tilde{H}_0	incident magnetic field

k	wavenumber
\tilde{n}	local surface normal
$\tilde{n}_A, \tilde{r}'_A, \tilde{e}_{r_A}$	normal unit vector, position vector and radial unit vector at a stationary phase point A
$r'(\theta, \varphi)$	surface equation
β	roughness parameter
δ	standard deviation of the rough surface
γ_C	angular roughness scale
ε_0, μ_0	free-space permittivity and permeability, respectively
ϕ	phase of the scattered field
$\phi_{\alpha\beta}$	phase difference between the signals of two point detectors α and β
$\phi_{\alpha\beta}^{sphere}$	phase difference which corresponds to an unperturbed sphere of radius a
$\langle \phi_{\alpha\beta} \rangle$	mean of the phase difference
(θ, φ)	polar angles
(θ_A, φ_A)	polar angles of the stationary phase point
$\rho(\gamma)$	autocorrelation function of the surface profile
σ_ϕ^2	variance of the phase difference
σ_n^2	variances of the random variables a_n and b_n

7 References

- [1] B. Michel: Statistical method to calculate extinction by small irregularly shaped particles. *J. Opt. Soc. Am. A* 12 (1995) 2471–2781.
- [2] J. I. Peltoniemi: Variational volume integral equation method for electromagnetic scattering by irregular grains. *J. Quant. Spectrosc. Radiat. Transfer* 55 (1996) 637–647.
- [3] E. Bahar, M. A. Fizwater: Scattering and depolarization by large conducting spheres with rough surface. *Appl. Opt.* 25 (1985) 1820–1825.
- [4] E. Bahar, M. A. Fizwater: Scattering and depolarization by conducting cylinders with rough surface. *Appl. Opt.* 25 (1985) 1826–1832.
- [5] R. Schiffer: The coherent scattering cross-section of a slightly rough sphere. *Opt. Acta* 33 (1986) 959–980.
- [6] G. A. Farias, E. F. Vasconcelos, S. L. Cesar, A. A. Maradudin: Mie scattering by a perfectly conducting sphere with a rough surface. *Physica A* 207 (1994) 315–322.
- [7] P. Beckmann, A. Spizzichino: *The Scattering of Electromagnetic Waves from Rough Surfaces*. Macmillan, New York 1963.
- [8] A. Ishimaru, J. S. Chen: Scattering from very rough surfaces based on the modified second-order Kirchhoff approximation with angular and propagation shadowing. *JASA* 88 (1990) 1877–1883.
- [9] K. Muinonen, T. Nousiainen, P. Fast, K. Lumme, J. I. Peltoniemi: Light scattering by Gaussian random particles: ray optics approximation. *J. Quant. Spectrosc. Radiat. Transfer* 55 (1996) 577–601.
- [10] M. Born, E. Wolf: *Principles of Optics*, 6th edn. Pergamon Press, Oxford 1980.
- [11] A. Doicu, T. Wriedt, K. Bauckhage: Light scattering by homogeneous axisymmetric particles for PDA-calculations to measure both axes of spheroidal particles. *Part. Part. Syst. Charact.* 14 (1997) 3–11.
- [12] G. Göbel, T. Wriedt, K. Bauckhage: Micron and sub-micron aerosol sizing with a standard phase-Doppler anemometer. submitted to *J. Aerosol Sci.* 26 (1997).
- [13] E. J. Davis: A history of single aerosol particle levitation. *J. Aerosol Sci.* 26 (1997) 212–254.
- [14] E. Bar-Ziv, A. F. Sarofim: The electrodynamic chamber: a tool for studying high temperature kinetics involving liquid and solid particles. *Prog. Energy Combust. Sci.* 17 (1991) 1–65.